Energy for Sustainability International Conference 2017
Designing Cities & Communities for the Future
Funchal, 8-10 February, 2017

EFFECTIVE HEAT CAPACITY METHOD TO SIMULATE HEAT DIFUSION PROBLEMS WITH PHASE CHANGE

N. Soares[1,2]*, P. Antunes[1], J.J. Costa[1]

1: ADAI, LAETA, Department of Mechanical Engineering, University of Coimbra, Coimbra, Portugal.
*e-mail: nelson.soares@dem.uc.pt
2: ISISE, Department of Civil Engineering, University of Coimbra, Coimbra, Portugal

Keywords: Phase change materials, PCM, Energy storage, Effective heat capacity.

Abstract *This paper presents the validation of a numerical model based on the effective heat capacity method to evaluate the heat transfer with melting/solidification of a microencapsulated phase change material (PCM) – Micronal® DS 5001 X – contained in rectangular-sectioned vertical cavities. In this method, the latent heat is modelled in the energy conservation equation as an artificially inflated specific heat within the temperature interval where phase change occurs. Due to the artificial nature of the method, particular attention is addressed to the variation of the effective (or equivalent) heat capacity with temperature in order to ensure a correct prediction of the phase change kinetics and the accurate quantification of the stored/released energy during a charging/discharging cycle of the PCM. Two variation functions were investigated: rectangular and triangular profiles. To validate the numerical results against experimental data from a preceding study, calculations were performed for three configurations of a small thermal energy storage (TES) unit, considering different boundary conditions that were specified in the numerical model as measured during the experiments. In the overall, numerical results show good agreement with experiments. However, it was concluded that the triangular function does not adequately reflect the time evolution of the phase change processes. Furthermore, it leads to a deficit in the latent heat that implies the use of a correction to accurately quantify the total energy stored/released by the PCM. With the appropriate correction, both the rectangular and the triangular approaches provide adequate predictions of the problem kinetics. These considerations must be taken into account in future applications of the effective heat capacity method.*

1. INTRODUCTION

PCMs are materials that undergo melting/solidification at a nearly constant temperature, storing/releasing great amounts of energy due to the latent heat involved in the solid-liquid phase change processes. Therefore, PCMs are very suitable for thermal management and TES applications. The incorporation of PCMs in small TES units (also called heat sinks) has been a subject of great interest and much work has been developed worldwide, as reviewed by Soares *et al.* [1]. These TES units are typically made of a high-conductivity internally-finned container used to accommodate the PCM and to overcome the low thermal conductivity of paraffins, commonly used as PCMs. To prevent liquid leakage, the metallic container can be the only way of containment, or the PCM can be further microencapsulated before filling the macrocapsule. The main advantage of using TES units filled with microencapsulated PCMs is that the problem of liquid leakage during manufacturing, assembling and operation can be significantly reduced. When dealing with microencapsulated PCMs, the numerical modelling of the heat transfer with phase change becomes simpler, as the advection phenomena in the melted domain can be neglected [2] and the energy conservation equation (in its purely diffusive form) is the only governing equation to be solved.

This paper presents a numerical model developed in a homemade FORTRAN program. The model is based on the effective heat capacity method to evaluate the heat transfer with melting/solidification of a paraffin-based microencapsulated PCM contained in rectangular cavities. The experimental results found in refs. [2,3] are used to validate the numerical model. The main goal of this work is to assess which kind of function (triangular or rectangular) for the variation of the effective heat capacity with temperature is more suitable to simulate the kinetics of the phase change processes and to determine the stored/released energy during a charging/discharging cycle. This work also aims to evaluate the influence of the aspect ratio of the cavities on the time required for completely melting the volume of PCM during charging, t_m, and for solidifying the PCM during discharging, t_s.

2. EXPERIMENTAL PROCEDURE AND PHYSICAL MODEL

Since the experimental data obtained by Soares *et al.* [2,3] will be used for the validation of the numerical model, including the measured temperatures on the surfaces of the TES unit which will be considered as dynamic boundary conditions in the numerical study, it is convenient to introduce beforehand the experimental procedure carried out by the authors. In the laboratory setup, the TES unit has a fixed position and it is thermally insulated on its upper and lower smaller faces, such that only the right and left square bigger surfaces will be thermally active. On its left side, a heating module holding a 68 W electrical resistance (the hot-plate) is tightly fixed to perform charging processes. During charging, a thermal insulation board is placed on the rear (right) side of the TES unit to ensure adiabatic conditions. To carry out discharging processes, a cooling module holding a heat exchanger fed by a thermo-regulated water flow (the cold-plate) is tightly placed on the right side of the TES unit. A thermal insulation board is then placed on the left side of the TES unit to ensure adiabatic conditions. Twenty-one K-type thermocouples are distributed

on the right and left surfaces of the TES unit, respectively, to record the time evolution of temperature on both faces. Five K-type thermocouples are also positioned on the mid-plane of the TES unit to measure the temperature evolution within the PCM domain. Data from all sensors are collected and stored at 30 s intervals. Further details about the experimental setup, instrumentation and procedure can be found in refs. [2] and [3].

Fig. 1a shows a sketch of the 1-single cavity TES unit whose central cross section is the 2D physical model considered in the simulations. In the numerical model, the boundary conditions imposed on the vertical surfaces reproduce the time evolution of the average temperature measured on the left and right faces of the TES unit during the experiments, $TH(t)$ and $TC(t)$ respectively. The top and bottom frontiers are set to be adiabatic. T_i (i = 1 to 5, from top to bottom) are the temperatures of the PCM measured in the mid-line of the central cross section of the TES unit. To evaluate the influence of the aspect ratio of the cavities during melting and solidification processes, as well as the influence of adding metallic fins, three different configurations of the TES unit are considered, as shown in Fig. 1, with the T_i temperatures measured or calculated at the same position in every configuration.

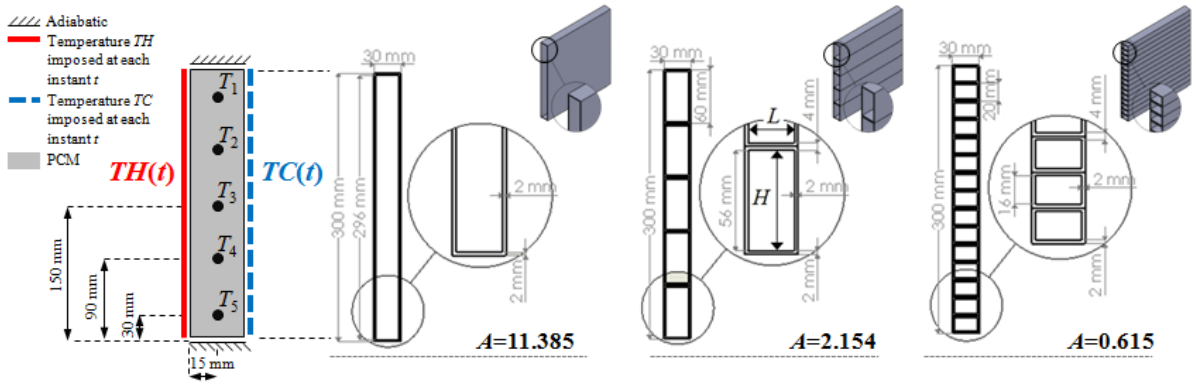

(a) (b) (c)

Figure 1. (a) Sketch of the physical model and imposed boundary conditions for the 1-single cavity TES unit (A=11.385). Sketch and dimensions of the TES units with (b) 5-cavities (A=2.154) and (c) 15-cavities (A=0.615).

3. MATHEMATICAL MODEL AND NUMERICAL SOLUTION

The just described boundary conditions of the physical model are considered in the numerical approach. The numerical model is based on the solution of the energy conservation equation, under purely diffusive conditions, and uses the effective heat capacity method to account for the latent heat of the solid-liquid phase change processes. The two-dimensional heat conduction equation with phase change, expressed in Cartesian coordinates can thus be written as:

$$\rho\, c_{eff}(T)\frac{\partial T}{\partial t} = \frac{\partial}{\partial x}\left(k\frac{\partial T}{\partial x}\right) + \frac{\partial}{\partial y}\left(k\frac{\partial T}{\partial y}\right). \quad (1)$$

The main feature of the effective heat capacity method is that the temperature is the only dependent variable to find. Moreover, the method allows using the same governing equation for both solid and liquid phases, avoiding the need to track the melting front position to solve the problem. Indeed, the melting/solidification fraction at each CV of the PCM domain (for each time step) is obtained as a function of the temperature calculated at the considered time step.

The key in the implementation of the method lies in the approximation used for the effective heat capacity term in Eq. (1). Three procedures are commonly used: the empirical, the numerical, and the artificial approximations. The former is used when detailed information about the thermal behaviour of the PCM is available and mathematical expressions $c_{eff}(T)$ are formed to approximate the heat capacity of the PCM. The second procedure also entails the knowledge of the thermal behaviour of the PCM, but in this case the evolution of the effective heat capacity of the PCM is determined numerically, for instance, using a derivative of enthalpy with respect to temperature. The latter procedure is used when limited data about the thermal behaviour of the PCM is known. This is the case of most of the commonly used paraffin-based commercial PCMs, as manufactures typically provide only the melting temperature, the latent heat of fusion and the specific heat of solid and liquid phases. As suggested by Al-Saadi and Zhai [4], such minimal data can be used to approximate the heat capacity of the PCM using a simple direct relationship with the introduction of a fictitious melting temperature range (ΔT_m), which is not known *a priori*. Figs. 2a and 2b sketch two different artificial approximations of the evolution of the effective heat capacity with temperature: the rectangular and the triangular functions. As shown in Figs. 2a and 2b, the latent heat of fusion is artificially approximated by a large effective heat capacity over the phase change temperature interval. In the numerical model, this high value of the effective heat capacity will block the increase (or decrease) of temperature during phase change.

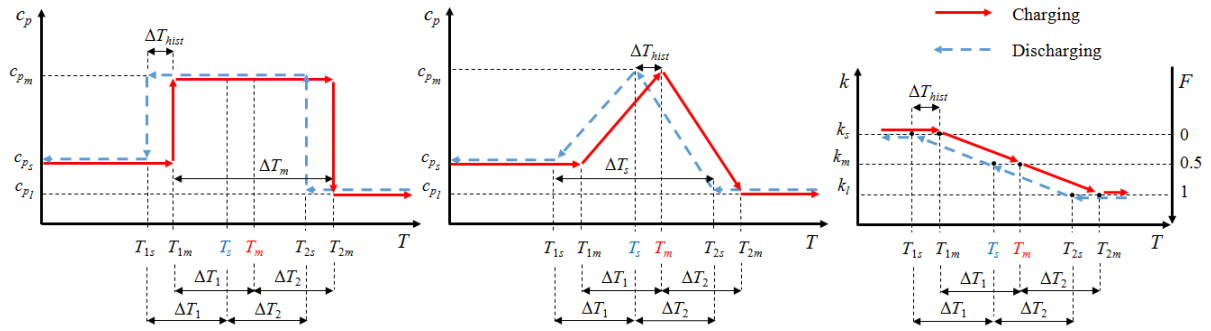

Figure 2. Sketch of the effective heat capacity method considering two artificial approximations for $c_{eff}(T)$: (a) rectangular and (b) triangular functions. (c) Sketch of the evolution of both the thermal conductivity, k, of the PCM and the fraction of melted PCM, F, with temperature.

Eqs. (2) and (3) present the definition of the effective heat capacity method for the phase change temperature interval during the charging process, for the rectangular and

triangular approximations, respectively. The c_{pm} term is given by Eq. (4), revealing that during phase change the effective heat capacity of the PCM is (or grows up) directly proportional to the latent heat L and inversely proportional to the temperature interval for phase change ΔT_m. T_{1m} is the temperature when the PCM begins melting and T_{2m} is the temperature when the PCM is completely melted. Additional information about the implementation of the effective heat capacity method can be found in ref. [5].

$$c_p(T) = \begin{cases} c_{p_s} & T \le T_{1m} \\ c_{p_m}, & T_{1m} < T < T_{2m} \\ c_{p_l} & T \ge T_{2m} \end{cases} \tag{2}$$

$$c_p(T) = \begin{cases} c_{p_s} & T \le T_{1m} \\ c_{ps} + \dfrac{c_{p_m} - c_{p_s}}{T_m - T_{1m}}(T - T_{1m}) & T_{1m} < T < T_m \\ c_{p_m} + \dfrac{c_{p_l} - c_{p_m}}{T_{2m} - T_m}(T - T_m) & T_m < T < T_{2m} \\ c_{p_l} & T \ge T_{2m} \end{cases}, \tag{3}$$

$$c_{p_m} = \frac{L}{\Delta T_m} + \frac{c_{p_s} + c_{p_l}}{2} \tag{4}$$

As pointed out by Liu *et al.* [6], the effective heat capacity method has difficulty in solving phase change problems when the phase change temperature range is small, and it is not applicable to the cases where phase change occurs at a fixed temperature. Al-Saadi and Zhai [4] have also remarked that small time steps and fine grids are required for accuracy. However, this method can easily deal with the supercooling phenomenon occurring during solidification. Fig. 2 shows the impact of hysteresis, ΔT_{hist}, in the two heat capacity approximations. In discharging processes, T_m must be replaced by T_s in Eqs. (2) and (3). Indeed, subscripts *m* and *s* refer to melting and solidification, respectively. Another important feature of this method is the flexibility to adjust the approximation of the effective heat capacity by considering different values of ΔT_1 and ΔT_2 (see Fig. 2). Furthermore, these values can be different for the charging and discharging processes.

The following assumptions are made in the present numerical model: (*i*) conduction is the only mode of heat transfer within the microencapsulated PCM domain; (*ii*) the thermophysical properties of the materials are independent of temperature, but for the PCM, c_p and k are different for the solid and liquid phases and k varies linearly with temperature during phase change (see Fig. 2c); (*iii*) the fraction of melted PCM at each CV, F, is a function of the calculated temperature (see Fig. 2c); (*iv*) the effect of expansion/contraction of the PCM during the phase change is neglected and a constant ρ-value is considered for both phases; (v) the materials are homogeneous and isotropic. The main thermophysical properties of the materials used are listed in Table 1.

The partial differential equation is discretized using the finite-volume method proposed by Patankar [7] with a fully implicit formulation. For the heat fluxes at the faces of each control volume (CV), the temperature gradients are approached by finite-

differences and the harmonic mean is used to interpolate the thermal conductivity values at the CV interfaces. A preliminary study was conducted to evaluate the influence of the time and spatial discretizations on the numerical solutions. Grid independence was declared when the variation of the total stored/released energy, E_1, between two consecutively refined grids (at a ½ size ratio) was lower than 0.1% and 1%, for the charging and discharging simulations, respectively. Time-step independence was recognized when the variation of the E_1-value was lower than 0.1% and 1.9% for the charging and discharging simulations, respectively, considering a time-step refinement ratio of 1.5. Finally, a regular mesh of 60 × 600 inner nodes (CV of 0.5 × 0.5 mm^2) was adopted for the calculations together with a time step of 10 s. The set of algebraic discretization equations is solved using a tri-diagonal matrix (TDMA) algorithm. At each time step, convergence is declared when the normalized sum of the absolute values of the residuals of the discretized equations is lower than 5×10^{-4}.

Table 1. Thermophysical properties of the materials.

	T_m [ºC]	ΔT_{hist} [ºC]	ρ [kg.m^{-3}]	L [kJ.kg^{-1}]	c_p [J.kg^{-1}.°C^{-1}]	k [W.m^{-1}.°C^{-1}]
PCM	25.7	1	995	110	2478 (solid) 1774 (liquid)	0.17 (solid) 0.15 (liquid)
Aluminium	–	–	2707	–	896	204

4. RESULTS AND DISCUSSION

To validate the numerical model, the calculated evolution of $T_{num}(t)$ in the mid-line of the central cross section of the TES unit will be compared to the time evolution of $T_{exp}(t)$ recorded during the experiments (subscripts i = 1 to 5 refer to the location of the thermocouples as sketched in Fig. 1). The total energy stored/released by the PCM during a charging/discharging cycle, E_1, will be calculated by integrating over time the instantaneous heat rate (per unit depth, Δz = 1m) in the interface aluminium-PCM. E_1 will be compared to the value of the stored/released energy during a complete charging/discharging cycle of the PCM, E_2, obtained by Eq. (5). E_2 is calculated based on the distribution of temperature in the PCM domain at the beginning and ending of simulations. In Eq. (5), $V_{i,j}$ is the volume of each CV occupied by the PCM, ρ is the density of the PCM (which is considered constant and equal for both phases), c_p is the specific heat and L is the latent heat of fusion. Subscripts s and l refer to the solid and liquid phases of the PCM, respectively. T_m is the melting temperature of the PCM, and T_{fin} and T_{ini} are the final and initial temperatures reached by the PCM at each CV (i,j), respectively.

$$E_2 = \sum_i \sum_j \rho_{i,j} \times V_{i,j} \times \left[c_{p_s} \left(T_{m_{i,j}} - T_{ini_{i,j}} \right) + L_{i,j} + c_{p_l} \left(T_{fin_{i,j}} - T_{m_{i,j}} \right) \right] \quad (5)$$

Fig. 3 shows the time evolution of $TH(t)$ and $TC(t)$, specified as boundary conditions during charging and discharging simulations of the 15-cavities TES unit, together with the $T_{3,exp}$ values measured during the charging and discharging experiments [2,3]. The time evolutions of $T_{3,num}$ calculated with different approximations of the

effective heat capacity are also presented for the charging and discharging simulations. The time evolutions of $T_{3,exp}$ and $T_{3,num}$ are compared to evaluate which method is more accurate to predict the kinetics of the phase change processes, and to assess the reliability of the numerical procedures. The numerical results were obtained by considering ΔT_1 = 5 ºC and ΔT_2 = 2 ºC for both the triangular and rectangular approximations (see Fig. 2). Table 2 presents the main results of the parametric study carried out to evaluate the influence of the aspect ratio of the cavities during charging and discharging.

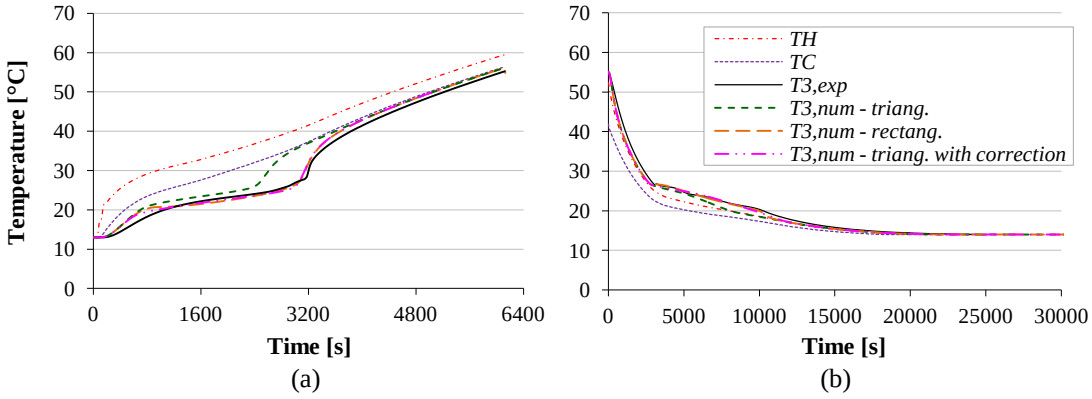

Figure 3. Time evolutions of the boundary conditions specified during (a) charging and (b) discharging simulations of the 15-cavities TES unit, and of $T_{3,num}$ calculated with different approximations of the effective heat capacity for the same tests cases, in comparison with with $T_{3,exp}$.

It can be seen from Figs. 3a and 3b that a good agreement between numerical results and experimental data was achieved for the rectangular profile of c_{eff}, in both charging and discharging simulations, which proves the reliability of the numerical method. However, for the triangular approximation, the PCM starts melting/solidifying too soon in comparison with the experimental data. This is caused by a deficit of latent heat during phase change, which is inherent to the approximation presented in Fig. 2b. To overcome this problem, the triangular approximation is corrected by doubling the L-value in Eq. (4).

Table 2. Main results of the parametric study carried out.

TES unit	A = 11.385			A = 2.154			A = 0.615		
Approximation method for $c_{eff}(T)$	Triang.	Triang. with correction	Rectang.	Triang.	Triang. with correction	Rectang.	Triang.	Triang. with correction	Rectang.
Charging									
E_1 [kJ]	335.1	455.9	454.1	324.1	430.9	429.7	259.4	360.8	360.1
E_2 [kJ]	460.5	457.4	457.4	433.6	432.2	432.2	362.1	362.1	362.1
t_m [s]	3680	4740	4750	3510	4540	4540	2490	3150	3160
Discharging									
E_1 [kJ]	320.2	440.4	445.2	309.2	398.7	421.4	257.7	356.7	356.6
E_2 [kJ]	431.3	431.3	431.3	408.0	408.0	408.0	349.7	349.7	349.7
t_s [s]	12270	18020	16620	9460	14170	13900	8630	11500	10310

Figs. 3a and 3b show that a good agreement between numerical results and experimental data is achieved with the corrected triangular profile of c_{eff} (ΔT_1 = 7 ºC and ΔT_2 = 2 ºC). The values listed in Table 2 also shows that similar results are achieved with both the rectangular and the corrected triangular approximations. Table 2 show that all the approximation profiles of c_{eff} can be used to determine E_2. This is particular interesting for the case of the triangular profile without correction, which however cannot be used to estimate E_1. To intuitively illustrate the phase change processes for the simulated cases and configurations, Figs. 4 and 5 show, respectively, the temperature and the melted fraction distributions at different moments of the melting and solidification processes.

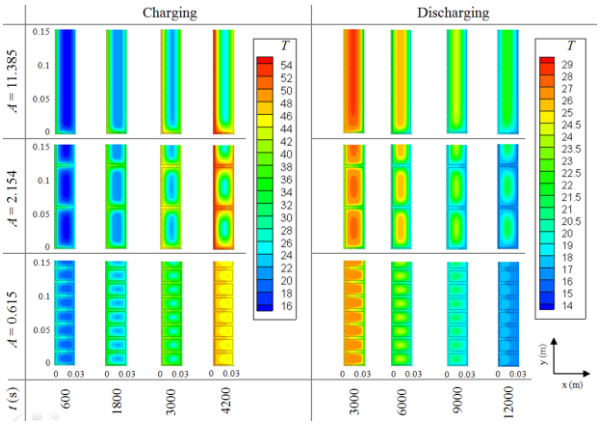

(a) (b)

Figure 4. Time evolution of the temperature distribution for different configurations of the TES unit during (a) charging and (b) discharging.

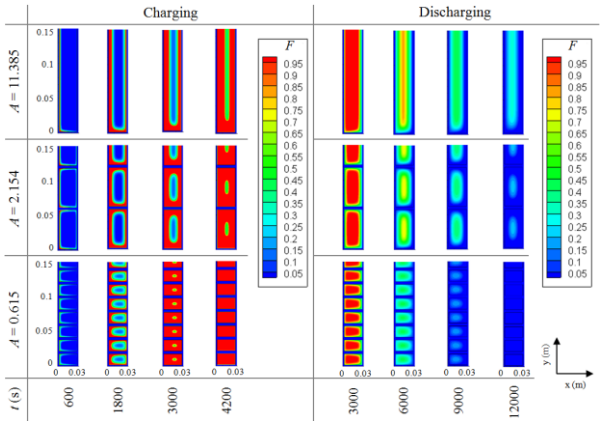

(a) (b)

Figure 5. Time evolution of the melted fraction distribution for different configurations of the TES unit during (a) charging and (b) discharging.

5. CONCLUSION

In this paper, previous experimental results were used to validate a homemade numerical model based on the effective heat capacity formulation. Two approximations of the effective heat capacity were investigated. Is was concluded that either the rectangular-profile approximation or the triangular-profile approximation, with appropriate correction, can be used with confidence in future simulations, as both functions reflect the kinetics of the phase change processes. Moreover, these approximation profiles can be used to properly estimate the stored/released energy by the PCM during a charging/discharging cycle. It was also concluded that the configuration of the TES unit plays an important role in the conduction-dominated phase change processes. As expected, the higher the number of metallic fins, the lower the time required for complete melting (or solidifying) the PCM during a charging (or discharging) process.

ACKNOWLEDGEMENTS

This project has been financed by FEDER funds through the COMPETE 2020-Operational

Programme for Competitiveness and Internationalization (POCI), and by Portuguese funds through FCT in the framework of the project POCI-01-0145-FEDER-016750 | PTDC/EMS-ENE/6079/2014.

REFERENCES

[1] N. Soares, J.J. Costa, A.R. Gaspar and P. Santos, "Review of passive PCM latent heat thermal energy storage systems towards buildings' energy efficiency", *Energy and Buildings* Vol. 59, pp. 82–103, (2013).

[2] N. Soares, A.R. Gaspar, P. Santos and J.J. Costa, "Experimental study of the heat transfer through a vertical stack of rectangular cavities filled with phase change materials", *Applied Energy* Vol. 142, pp. 192–205, (2015).

[3] N. Soares, A.R. Gaspar, P. Santos and J.J. Costa, "Experimental evaluation of the heat transfer through small PCM-based thermal energy storage units for building applications", *Energy and Buildings* Vol. 116, pp. 18–34, (2016).

[4] S.N. AL-Saadi and Z.(J.) Zhai, "Modeling phase change materials embedded in building enclosure: a review", *Renewable and Sustainable Energy Reviews* Vol. 21, pp. 659–673, (2013).

[5] P. Antunes, *Estudo numérico de unidades de armazenamento de energia térmica com materiais de mudança de fase para a termorregulação de painéis fotovoltaicos*, Master thesis in Mechanical Engineering, Universidade de Coimbra, (2016).

[6] S. Liu, Y. Li and Y. Zhang, "Review on heat transfer mechanisms and characteristics in encapsulated PCMs", *Heat Transfer Engineering* Vol. 36 (10), pp. 880–901, (2015).
S.V. Patankar, *Numerical heat transfer and fluid flow*, Washington, DC: Hemisphere Publishing Corporation, (1980).